Numerical Calculation of Inclusive Spectra and Correlations in a φ^3 Ladder Model*

Fritz W. Bopp
Physics Department, University of Illinois at Urbana-Champaign, Urbana, Illinois 61801
(Received 5 November 1971)

We present a numerical calculation of the inclusive one- and two-particle spectra and the two-particle correlation function at several energies for ladder diagrams in a $\lambda\varphi^3$ field theory.

I. INTRODUCTION

At presently available accelerator energies the inelastic contributions to the scattering cross section are dominant; however, the complexity of many-particle production processes makes them not immediately amenable to many of the techniques used in two-body reactions. Thus the understanding of high-multiplicity events requires new methods and models. In view of the presumably complicated underlying physical situation, Wilson[1] has suggested that the aim of the new models should be to explain the gross qualitative features, which hopefully reflect only the dominant physical effects. Instead of studying all final-state particles one should deal only with highly integrated quantities. Such quantities are the total cross section, the contributions of special multiplicity channels, and the inclusive one- and two-particle spectra. In this paper, the inclusive spectra will be of central interest.

For the purpose of analysis the spectra can be divided kinematically into regions called "fragmentation" and "pionization." As the boundary between these two regions is controversial,[2] let us state our definition of these terms. Common to all definitions are two features: (1) The pionization and the fragmentation are complementary parts of the spectrum, and (2) the fragmentation consists of fragments of the target and fragments of the projectile which have momenta "comparable" to the initial momenta of, respectively, the target and the projectile. The exact mathematical definition of "comparable" is still moot. For simplicity we treat always the case in which all particles have the same mass. To formulate our definition let us first define the "plus" and "minus" components of a momentum vector and the "transverse mass,"

$$p^{\pm} = p_0 \pm p_{\parallel}, \quad m_{\perp} = (m^2 + p_{\perp}^2)^{1/2}. \tag{1}$$

We consider in the center-of-mass system the ratio of the plus or minus component of a momentum and its transverse mass,

$$r^{\pm} = p^{\pm}_{\text{c.m.}}/m_{\perp}.$$

If r^+ exceeds a constant fraction, η, of its maximum allowed value, we shall call the secondary a fragment of the projectile. Further, if r^+ is smaller than a fixed multiple of its minimum value – so that r^- is larger than a constant fraction of its maximum value – then we shall consider the secondary to be a fragment of the target. In the center-of-mass system we have the following division:

$$\begin{aligned} r^+_{\text{projectile}}\,[\approx (s/m^2)^{1/2}] & \\ > r^+_{\text{fragmentation projectile}} & > \eta r^+_{\text{projectile}} \\ > r^+_{\text{pionization}} & > \frac{1}{\eta} r^+_{\text{target}} \\ > r^+_{\text{fragmentation target}} & > r^+_{\text{target}}\,[\approx (m^2/s)^{1/2}]. \end{aligned} \tag{2}$$

Here η is a constant less than 1 but independent of s, say 0.1. Campbell and Chang show in an analytic calculation[3] that such a division is suggested by the multiperipheral model. As a slight change which does not alter their arguments, the transverse mass is included here to achieve a more symmetric form. Some features of our definition seem to be clearer in the rapidity space. The rapidity of a secondary is defined as $z = \ln r^+$; our definition gives a finite range in the rapidity space to the fragmentation regions, while the range of the rapidities of the pionization region grows with $\ln s$. The regions in this variable are given in expression (3):

$$\begin{aligned} z_{\text{projectile}} & > z_{\text{fragmentation}} > z_{\text{projectile}} - \text{const} \\ & > z_{\text{pionization}} > z_{\text{target}} + \text{const} \\ & > z_{\text{fragmentation}} > z_{\text{target}}, \end{aligned} \tag{3}$$

where

$$\text{const} = \ln(1/\eta).$$

These relations are invariant under longitudinal boost since such Lorentz transformations correspond to simple translations in the rapidity space. The division allows a simple interpretation of the empirical result $\langle n \rangle = A \ln s + B$. The term $A \ln s$ comes from the pionization region – in which, by Feynman's scaling hypothesis, the spectrum is as-

sumed to have an essentially constant height as a function of rapidity – and the term B represents the constant contribution from the fragmentation regions.

Current theoretical investigations[3] suggest that in the fragmentation region the secondary spectra depend on the initial particles; on the other hand, the pionization products are believed to be roughly independent of the beam and the target. Therefore, in seeking a first understanding of gross features common to all multiparticle production processes, we shall concentrate primarily on pionization products. In the pionization region, however, it appears to be difficult to distinguish clearly between existing models, as many models give total cross section, multiplicities, and one-particle inclusive longitudinal spectra all in rough agreement.

To differentiate between the models one must either go to quantitative considerations or look for quantities which contain more detailed, model-dependent information. The main purpose of this paper is to investigate such new quantities in a simple $\lambda\varphi^3$ multiperipheral model. We shall concentrate on the one- and two-particle inclusive spectra and on the two-particle correlation function.

A second purpose of this investigation is to test the results of existing calculations[4] (which use approximations like the neglect of transverse momenta and the assumption of infinite initial energy) with an unbiased and roughly accurate Monte Carlo integration. This comparison will be limited in most cases to the qualitative behavior, since the present calculation uses only the rather simplified $\lambda\varphi^3$ model.

The remainder of the paper is divided into two parts. Section II contains a detailed description of the model in which the calculation was done, while Sec. III presents the results of the calculations, dealing first with the general features and the one-particle inclusive spectrum and then with the two-particle inclusive spectrum and the two-particle correlation function.

II. THE MODEL AND THE APPROXIMATION USED IN THE CALCULATIONS

The present calculation is based on the ladder model in a $\lambda\varphi^3$ field theory; the corresponding Feynman diagrams are shown in Fig. 1(a). All particles, including the incoming ones, are spinless and have masses equal to the pion mass; there are no restrictions from the odd parity of the pions, and all additive quantum numbers are likewise neglected. For reasons which will be discussed later only ordered momenta of the secondaries are considered. This simplified model leads to the following expression:

$$\sigma = \sum_{n=2}^{\infty} (\lambda^2)^n \frac{1}{n!} \int_{\text{ordered momenta}} d\varphi_n \prod_{i=1}^{n+1} \frac{1}{(q_i^2 - m^2)^2}, \quad (4)$$

where $d\varphi_n$ denotes the appropriate phase space.

The Monte Carlo integration used here is described in a paper by Kittel, Van Hove, and Wójcik.[5] A short description of some details of the calculation is given in the Appendix.

The exact calculation has to be symmetrized over final states, as shown in Fig. 1(b). The biggest contribution comes from amplitudes in which the plus components of the momenta of the secondaries are ordered in the same way as their position in the chain. The product of two amplitudes with different permutations cannot satisfy the above condition in both factors. Neglecting such mixed contributions (interference terms) is a standard approximation in analytic calculations and its effect has been investigated by Snider and Tow[6] and Wyld.[7] It will cause a sizable quantitative change of the total cross section, as the number of nonleading terms rises rapidly, but more qualitative features like the height of the intercept of the

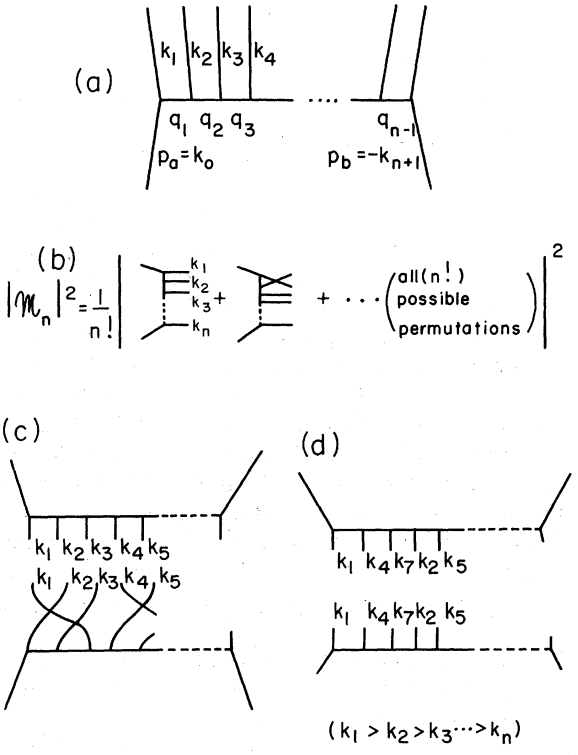

FIG. 1. (a) Feynman graph used. (b) The requirement to symmetrize over the final states. (c) Example of interference term not considered. (d) Example of other nonordered term not considered.

trajectory seem only slightly changed.[6] In addition squares of amplitudes with identical but nonordered permutations are neglected, as both factors should be small and such contributions should be less crucial than the neglected interference terms described above. Examples of Feynman graphs of both neglected types are given in Figs. 1(c) and 1(d).

The approximations are essential for numerical treatment of higher multiplicities. If we randomly include events with nonordered amplitudes, there will be roughly one ordered event with a sizable contribution in a total of $n!$ events; from $n!$ calculations one would obtain, therefore, essentially only one significant Monte Carlo event, a fact which makes the integration statistically unfeasible. Importance sampling for the selection of contributing permutations might improve the situation, but the present calculation avoids this complication.

III. RESULTS OF THE CALCULATION

Multiplicities

The contributions from channels with different multiplicities are given in Fig. 2(a) for the incident-beam laboratory momenta of 9, 90, and 900 GeV/c. These values have to be seen in relation to the chosen mass of the particles, i.e., the pion mass. We give therefore the invariant energy over mass squared,

$$s/m^2 = 130, 1300, 13\,000 .$$

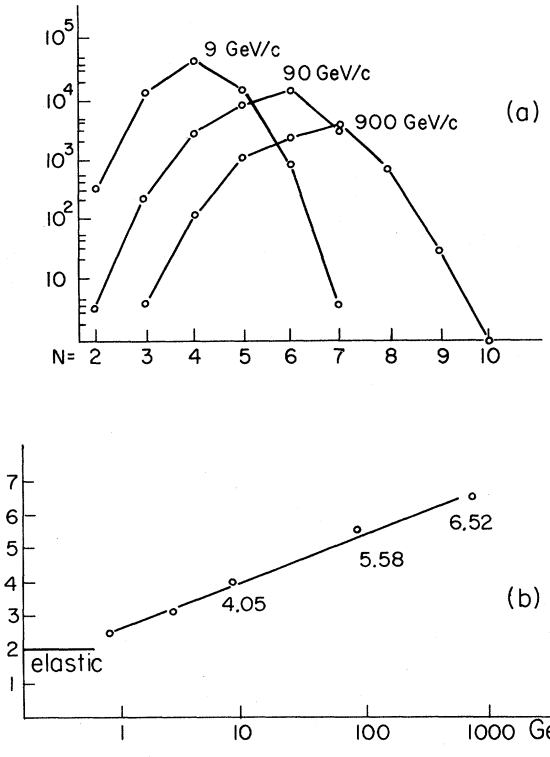

FIG. 2 (a) Contributions to different multiplicity channels. (b) Energy dependence of average multiplicity $\langle n \rangle$.

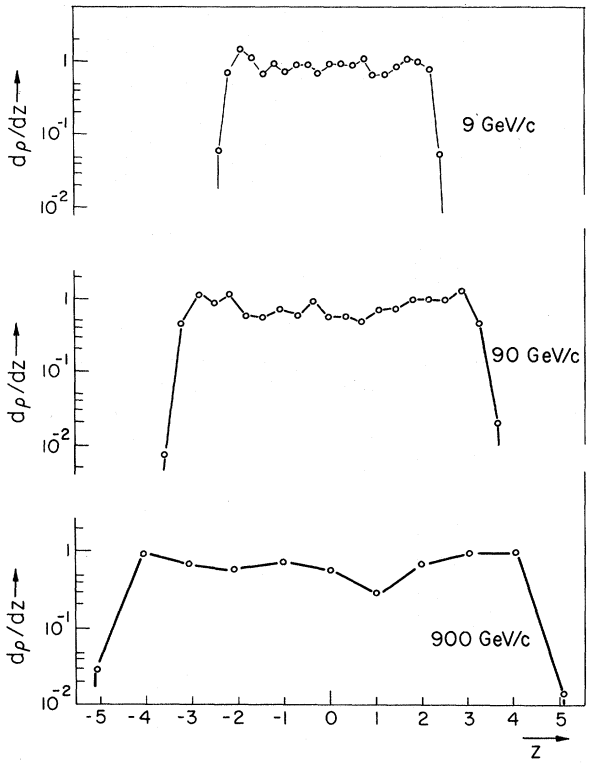

FIG. 3. Rapidity dependence of one-particle spectrum.

The leading multiplicity channels are so dominant that we have standard deviations $\langle (\Delta n)^2 \rangle$ of only 0.4, 0.8, and 0.8, respectively. These low values might suggest that the standard deviation has to fluctuate with increasing energy, i.e., that it has to rise slightly during a transition from one dominant multiplicity to another, when the two leading channels are about equally contributing. The distribution is not a Poisson distribution; even its first binomial moment $\langle (\Delta n)^2 \rangle - \langle n \rangle$ does not vanish. This is expected in the literature[8] and attributed to the existence of correlations. The fact that it does not even vanish approximately seems a special feature of the $\lambda\varphi^3$ multiperipheral model related to the above-mentioned dominance of the leading multiplicity channel.

Figure 2(b) gives the energy dependence of the average multiplicity. The values obtained lie approximately on a straight line with a slope of 0.6 and therefore we have approximately $\langle n \rangle = 0.6 \ln s + \text{const}$.

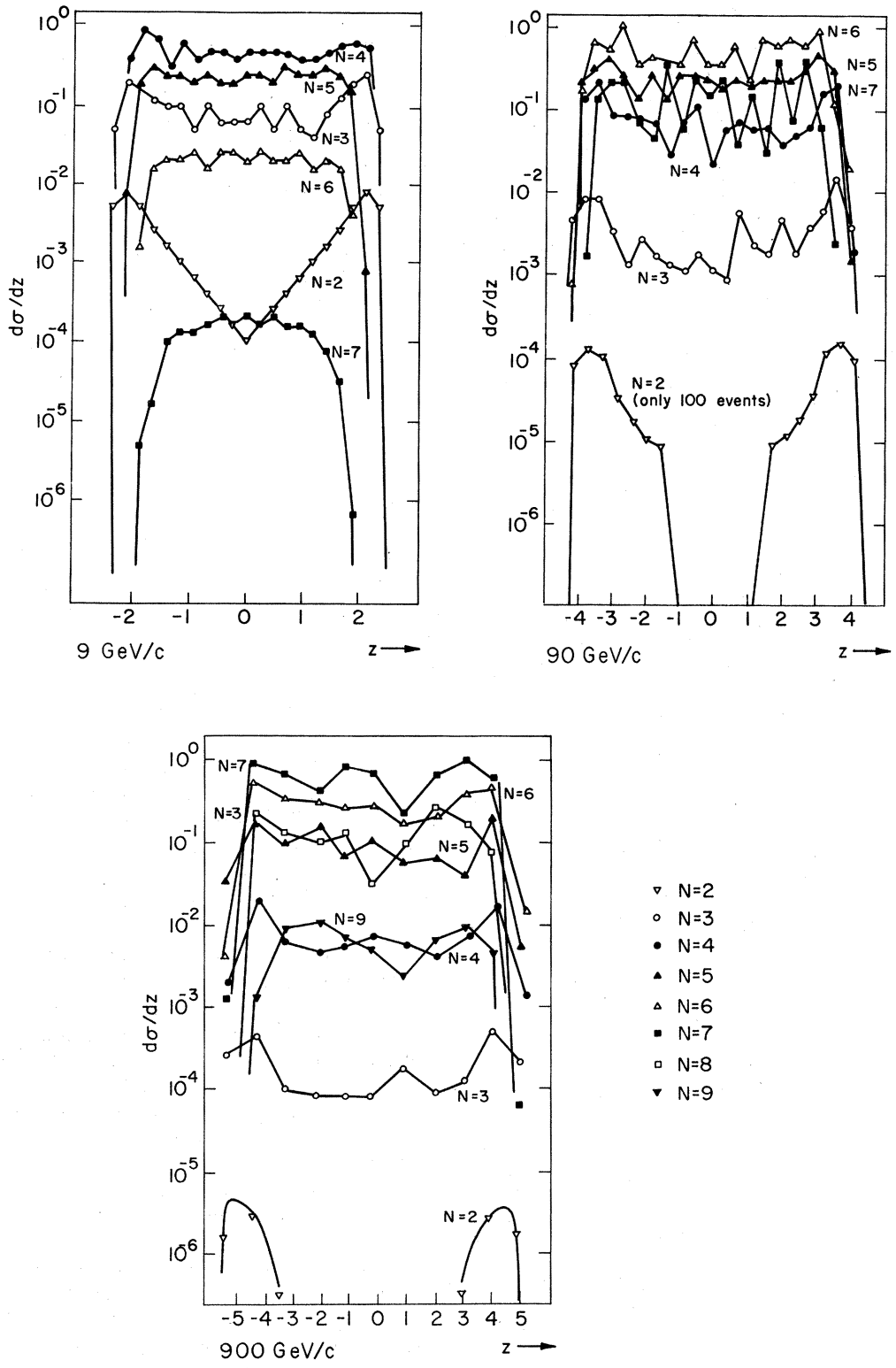

FIG. 4. Contributions of different multiplicity channels to the one-particle spectrum.

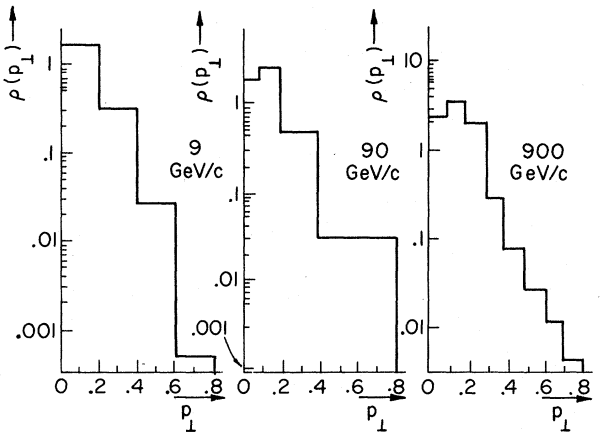

FIG. 5. Transverse-momentum dependence of one-particle spectrum.

One-Particle Spectrum

The aspect of the one-particle spectrum most thoroughly investigated theoretically is its dependence on the longitudinal momentum. Following Wilson we use the rapidity as the most suitable coordinate for examining this dependence. The spectrum $\rho(z) = (d\sigma/dz)(1/\sigma)$ resulting from our model is given in Fig. 3 for the three momentum values mentioned above. It agrees qualitatively with the standard prediction, based on the gas analogy of the multiperipheral model, that there should be a relatively constant central region corresponding to pionization events. The origin of the form of the spectrum can be studied in Fig. 4 which shows the individual contributions to the one-particle spectrum of channels with different multiplicities. The relative size from different multiplicity channels is determined by the coupling constant λ; we have chosen this parameter such that the total cross section becomes roughly constant at higher energies ($\lambda^2 = 48.0$).[7] However, the obvious oversimplification inherent in a simple ladder model suggests that we should not adhere too rigidly to this value of the coupling constant and that we should perhaps investigate the effect of variations in its size. We did such an investiga-

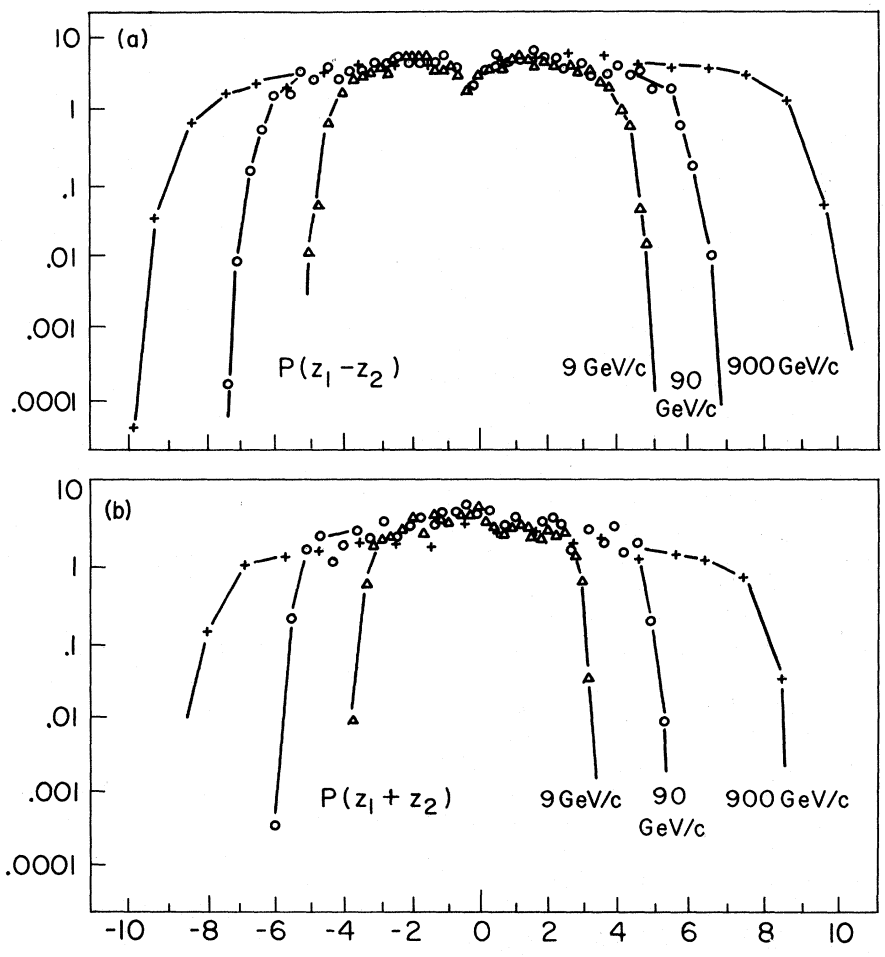

FIG. 6. The two-particle spectrum ($z_1 - z_2$ and $z_1 + z_2$ dependence separately).

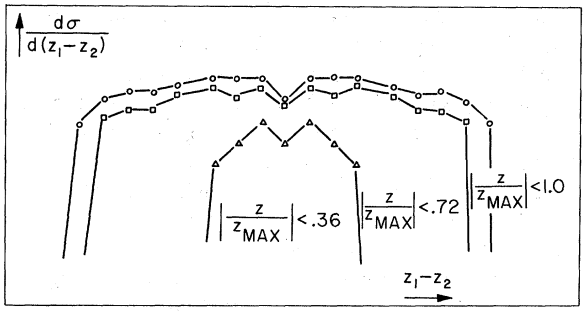

FIG. 7. Influence of cutoffs in large rapidities on the $z_1 - z_2$ dependence of the two-particle spectrum.

tion in a range from $\lambda^2 = 36.0$ to $\lambda^2 = 60.00$ and we found no noticeable change of the shape of the spectrum.

Figure 5 gives the dependence of the spectrum on the absolute value of the transverse momenta. We investigated the combined $(z, |p_\perp|)$ dependence of the spectra and found that the transverse-momentum dependence of the spectrum is roughly independent of z in the pionization region. This is again in agreement with theoretical arguments which suggest that in the pionization region $\rho(z, p_\perp) \to \rho(p_\perp)$.

Two-Particle Spectrum

The main interest in the present calculation lies in the two-particle spectrum,

$$P((z_1, p_1^\perp), (z_2, p_2^\perp)) = \frac{1}{\sigma} \frac{d^2\sigma((z_1, p_1^\perp), (z_2, p_2^\perp))}{d(z_1, p_1^\perp) d(z_2, p_2^\perp)}, \quad (5)$$

and, in particular, in its correlated part. As suitable coordinates in which to study these quantities we use the transverse momenta of the two particles and the sum and the difference of their rapidities. Feynman's gas analogy[1] suggests that the difference of the rapidities should contain all dynamical information and that the spectrum should have only a simple purely kinematical dependence on the sum of the rapidities. Figure 6(a) gives the $z_1 - z_2$ dependence of the spectrum. One finds a dip, which does not appear too sizable in this logarithmic plot, but which clearly exceeds the size of the random structure in the $z_1 + z_2$ dependence of the spectrum [Fig. 6(b)]. The complicated fragmentation region with its strong z dependence might disturb the simple gas-analogy picture. In general we did not attempt to exclude this region by cutoffs in $|z|$, as it seemed not possible to do so without introducing bias and not necessary for a qualitative study. The effect of such cutoffs is investigated in Fig. 7, the dip becomes somewhat clearer. The reason can be studied in Fig. 8 which shows the simultaneous dependence of P on both $z_1 + z_2$ and $z_1 - z_2$. The limited number of events allows only a small number of bins without loss of sufficient statistics. For the two-parameter dependence we have therefore used larger intervals in both rapidities. With a somewhat optimistic eye one can see a central region in which the spectrum is more or less only a function of $z_1 - z_2$ and which contains a small dip, which is somewhat washed out by the large integration intervals. The dip disappears for large $z_1 + z_2$ values, which have still a large contribution. In the integrated $z_1 - z_2$ spectrum without exclusion of the fragmentation region by cutoffs in large $|z|$ values, the relative size of the dip will therefore be lessened by this flat $z_1 - z_2$ distribution for large $z_1 + z_2$.

Correlation Function

One problem in the investigation of many-particle spectra is to separate dynamical correlations from statistical and kinematic effects. To extract most efficiently the new information contained in the two-particle spectrum one can simply subtract from it an uncorrelated two-particle spectrum obtained from the one-particle spectrum. In the standard way one can define

$$g(\vec{p}_1, \vec{p}_2) = P(\vec{p}_1, \vec{p}_2) - \rho(\vec{p}_1)\rho(\vec{p}_2). \quad (6)$$

The only important known structure in the $z_1 + z_2$ dependence of the correlation function should come from the momentum conservation which suppresses two large rapidities with equal sign. The structure of g in $z_1 - z_2$ depends critically on the dynamics of the model.[9] Most models predict that it disappears for large $z_1 - z_2$ values, but the sign and the size of the correlation at $z_1 - z_2 = 0$ should provide one of the most significant experimentally accessible facts about many-particle processes.

The correlation function resulting from our calculation is shown in Figs. 9 and 10 which give the dependence of g on $z_1 - z_2$ (integrated over $z_1 + z_2$) and, for comparison, the dependence on $z_1 + z_2$ (integrated over $z_1 - z_2$). The expected dip in $z_1 - z_2$ is now clearly the dominant feature. The fact that the correlation function does not disappear for large $z_1 - z_2$ values at 9 GeV/c can be attributed to kinematic effects which are still strong at this relatively low energy. The asymmetry in the $z_1 + z_2$ dependence is due to fluctuations and is actually useful in that it indicates the size of these fluctuations; the asymmetry in $z_1 - z_2$ is due to the fact that each pair of momenta is counted in both orders.

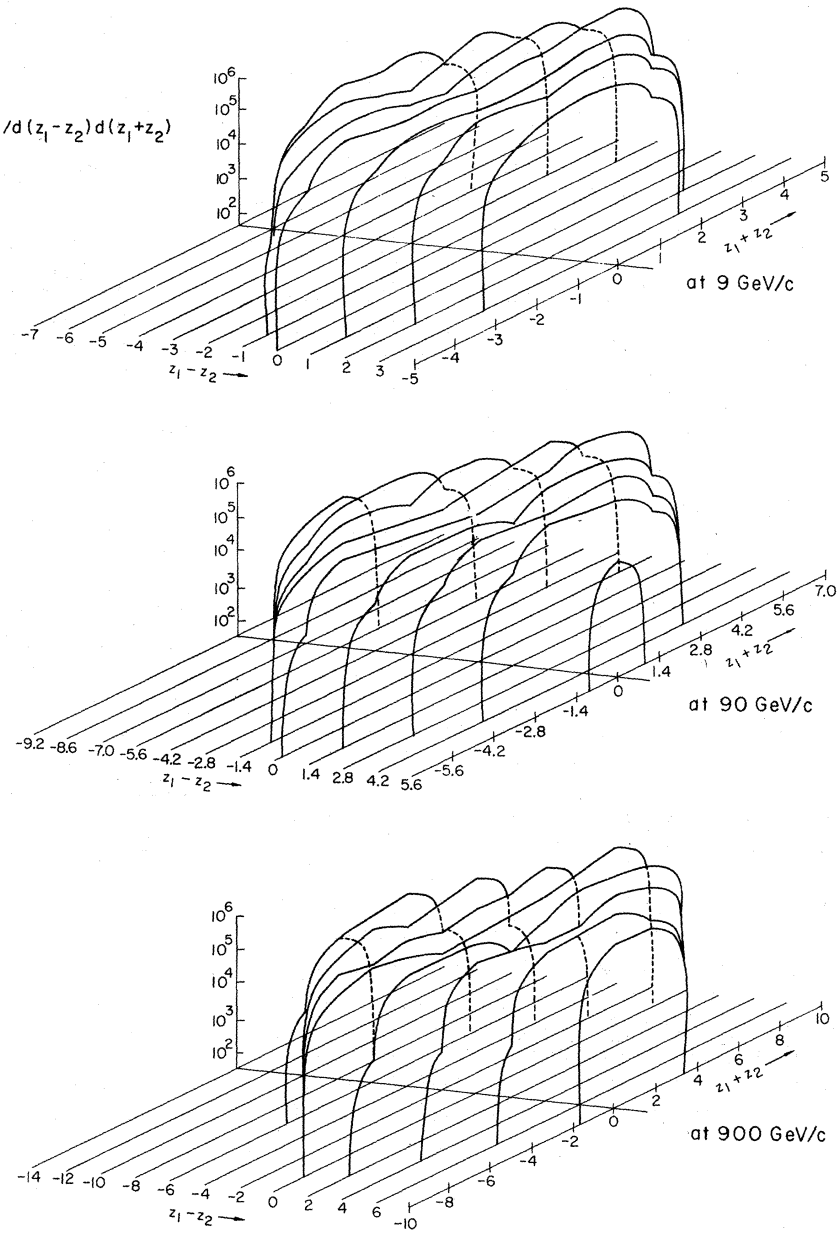

FIG. 8. The two-particle spectrum (z_1-z_2 and z_1+z_2 in one plot).

For reasons described above we varied again the coupling constant. Our result is shown in Fig. 11. The effect of this variation is not especially strong and the fact that the correlation decreases with weaker coupling constant is in agreement with the literature.[8]

Valuable information seems to be contained in the transverse-momentum dependence of the longitudinal correlation. We have investigated the influence of restrictions in the admitted transverse momenta and picked up for this purpose several cutoffs in the maximal allowed values of

$$\max(p_1^\perp, p_2^\perp) \quad \text{and} \quad |p_1^\perp - p_2^\perp| .$$

The expression for the correlation function contains the one- and two-particle spectrum and the total cross section. To avoid having to calculate for each cutoff an extra total cross section and an extra spectrum (this would be especially complicated as the cutoffs depend on pairs of secondaries), we used the following function as a substitute for the correlation function:

$$\tilde{g}(z_1, z_2) = P(z_1, z_2) - \tilde{p}(z_1)\tilde{p}(z_2) ,$$

where

$$\tilde{p}(z) = \int dz' P(z, z')$$

and where $P(z_1, z_2)$ is the normal two-particle

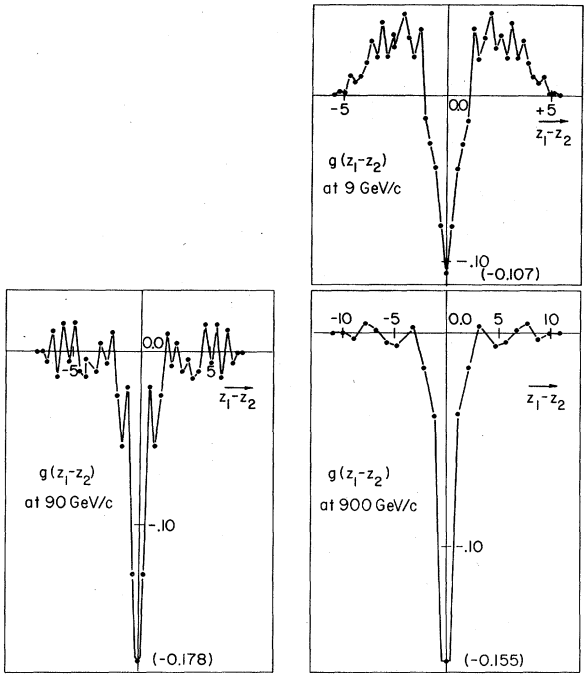

FIG. 9. The $z_1 - z_2$ dependence of the correlation function.

spectrum. It seems plausible that the dip in this function changes in the same way as the dip in the true correlation function. The result of this calculation is shown in Figs. 12(a) and 12(b). Restrictions in the transverse momenta increase the dip in the longitudinal correlation. The simple presence of large transverse momenta might lessen the structure in this longitudinal correlation or there might be an additional correlation in the transverse momenta for secondaries with comparable longitudinal momenta. The fact that cutoffs in $p_1^{\perp} - p_2^{\perp}$ seem to have a little stronger effect favors the second explanation.

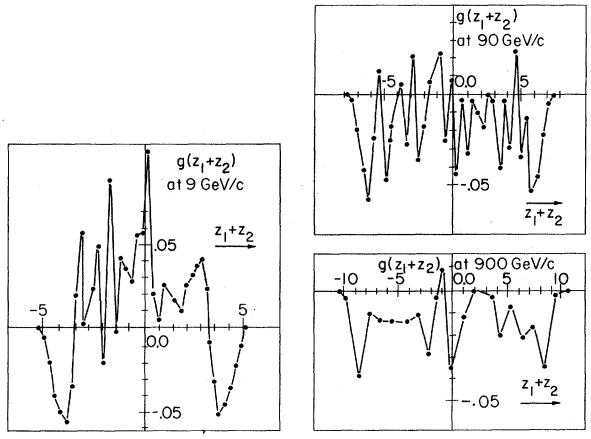

FIG. 10. The $z_1 + z_2$ dependence of the correlation function.

REMARKS

The paper contains a Monte Carlo integration of ladder diagrams. The advantage of this method of numerical integration is its flexibility in regard to the questions asked; its disadvantage is the relatively high statistical error. The number of bins in which the resulting spectra are divided is chosen large enough so that some obviously statistical fluctuations are not washed out and one obtains in this way a rough estimate of the size of the error.

As far as the results are concerned, we would like to place particular emphasis on the dip in the two-particle correlation function (Fig. 9). Qualitative arguments suggest that the existence of this dip does not depend on the details of the φ^3 ladder model, but is rather a general feature of any model of the general type in which the amplitude falls off rapidly with large momentum transfers. To show the basic idea let us consider the simplest case with two nonleading secondaries. Let us neglect transverse momenta and assume that the ratio of the outermost transfer momenta q_1^+/q_3^+ is much larger than one. Using momentum conservation we can obtain the following equations:

$$q_1^2 + \mu^2 - q_2^2 = q_1^2 \frac{k_2^+}{q_1^+} + \mu^2 \frac{q_1^+}{k_2^+}$$

and

$$q_2^2 - \mu^2 - q_3^2 = q_3^2 \frac{k_3^+}{q_3^+} + \mu^2 \frac{q_3^+}{k_3^+} .$$

Treating separately the cases in which the ratios k_2^+/q_1^+ and k_3^+/q_3^+ are smaller and greater than one,

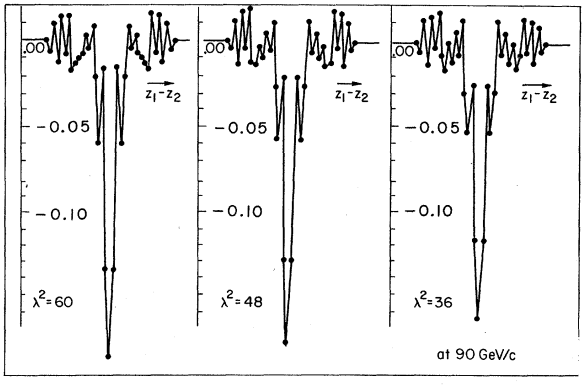

FIG. 11. Influence of variations in the coupling constant on the $z_1 - z_2$ dependence of the correlation function.

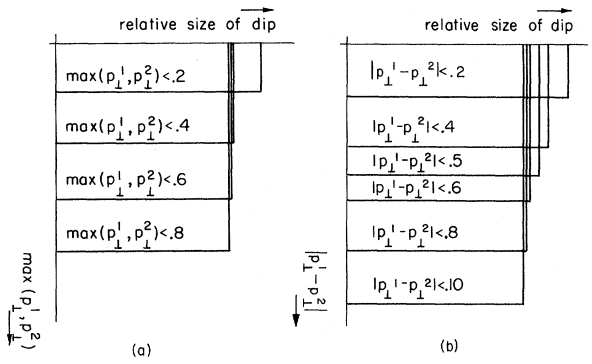

FIG. 12. (a) Influence of cutoffs in $\max(p_1^\perp, p_2^\perp)$ on the size of the dip in the $z_1 - z_2$ dependence of the correlation function. (b) Influence of cutoffs in $|p_1^\perp - p_2^\perp|$ on the size of the dip in the $z_1 - z_2$ dependence of the correlation function.

and assuming $q_3^2, q_1^2 \sim O(\mu^2) > 0$, we find lower and upper bounds on the ratios which depend only on masses and momentum transfers. From these restrictions on q_3^+/k_3^+ and k_2^+/q_1^+ we conclude that the ratio k_2^+/k_3^+ is large. Similar rapidities for two different secondaries are therefore unlikely and the correlation function has to have a negative dip at $z_1 - z_2 = 0$. The assumptions made can be justified by similar arguments and the argument generalized to an arbitrary number of final particles.

Our calculation gives the actual size and shape of this dip in a particular model.

ACKNOWLEDGMENTS

The author wishes to thank Professor H. W. Wyld, Professor S.-J. Chang, and especially Dr. D. K. Campbell for many helpful suggestions and interesting discussions.

APPENDIX

Some Technical and Numerical Details of the Calculation

A subroutine of the type described by Kittel, Van Hove, and Wójcik[5] generates randomly center-of-mass momenta in the available phase space. It distinguishes between transverse and longitudinal momenta and the known rapid decrease of the amplitude in the transverse momenta is taken into account by importance sampling. The result of the subroutine is a set of momenta with a weight factor. In distinction to Ref. 5 we have considered only strong ordering; therefore we have to sort the momenta according to their longitudinal components and to multiply the weight by the probability of such an ordering.

The subroutine belongs to the first part of a program which writes the momenta and weights on a disk, together with an amplitude calculated in a straightforward way from these parameters. A second step sums the contributions of these events into large arrays which contain the one- and two-particle spectra. In a third step we calculate from these arrays the integrated spectra and the correlated function. Only the last part has to be repeated for most of the different parts of the analysis. All steps were done for $p_2 = 9.0$, 90.0, and 900.0 GeV/c with more than 30 000 events for each momentum.

---

*Work supported in part by the National Science Foundation under Grant No. NSF GP 25303.

[1]K. Wilson, Cornell University Report No. CLNS-131, 1970 (unpublished); R. P. Feynman, Phys. Rev. Letters 23, 1415 (1969).

[2]J. P. Hsu, Phys. Rev. D 3, 257 (1971).

[3]D. K. Campbell and S.-J. Chang, Phys. Rev. D 4, 1151 (1971); 4, 3658 (1971); University of Illinois Report No. ILL-(TH)-71-10, 1971 (unpublished).

[4]C. E. DeTar, Phys. Rev. D 3, 128 (1971), and many other references.

[5]W. Kittel, L. Van Hove, and W. Wójcik, Computer Phys. Commutations 1, 425 (1970).

[6]D. R. Snider and D. M. Tow, Phys. Rev. D 3, 996 (1971).

[7]H. W. Wyld, Jr., Phys. Rev. D 3, 3090 (1971).

[8]A. H. Mueller, Phys. Rev. D 4, 150 (1971).

[9]S.-J. Chang, T.-M. Yan, and Y.-P. Yao, Phys. Rev. D 5, 271 (1972).